Available online at www.sciencedirect.com
SCIENCE DIRECT®
Bioorganic & Medicinal Chemistry Letters 14 (2004) 3697–3703
Bioorganic & Medicinal Chemistry Letters

Inhibition of monoamine oxidases by coumarin-3-acyl derivatives: biological activity and computational study

Franco Chimenti,[a] Daniela Secci,[a,*] Adriana Bolasco,[a] Paola Chimenti,[a] Arianna Granese,[a] Olivia Befani,[b] Paola Turini,[b] Stefano Alcaro[c] and Francesco Ortuso[c]

[a]*Dipartimento di Studi di Chimica e Tecnologia delle Sostanze Biologicamente Attive, Università degli Studi di Roma 'La Sapienza', P.le A. Moro 5, 00185 Rome, Italy*
[b]*Dipartimento di Scienze Biochimiche 'A.Rossi Fanelli' and Centro di Biologia Molecolare del CNR, Università degli Studi di Roma 'La Sapienza', P.le A. Moro 5, 00185 Rome, Italy*
[c]*Dipartimento di Scienze Farmaco Biologiche 'Complesso Ninı Barbieri', Università di Catanzaro 'Magna Graecia', 88021 Roccelletta di Borgia (CZ), Italy*

Received 25 February 2004; revised 21 April 2004; accepted 7 May 2004
Available online 2 June 2004

Abstract—A series of coumarin-3-acyl derivatives have been synthesized and investigated for the ability to inhibit selectively monoamine oxidases. The coumarin-3-carboxylic acids, **2a**–**e**, proved to be reversible and selective inhibitors of the MAO-B isoform, displaying pIC_{50} values of particular interest: **2a** shows pIC_{50} 7.76 and a selectivity index (pS.I.) 2.94 and **2b** shows pIC_{50} 7.72 and a pS.I. of 2.80. The coumarin-3-acyl chlorides **3a**–**e** showed high pIC_{50} values against both MAO-A and MAO-B isoforms, **3d** being the highest against MAO-B with a pIC_{50} value of 8.00. In order to rationalize the activity/selectivity results, molecular descriptors were generated. Further insight about enzyme–inhibitor interaction was obtained by docking experiments with the MAO-B isoform.

1. Introduction

Monoamine oxidase (MAO, EC 1.4.3.4) is a FAD-containing enzyme tightly bound to the mitochondrial outer membranes of neuronal, glial, and other cells.[1] It catalyzes the oxidative deamination of monoamines both from endogenous and exogenous sources, thereby affecting the concentrations of neurotransmitter amines as well as many xenobiotic[2] ones.

Two subtypes, MAO-A and MAO-B, which have a different inhibitor, amino acid sequence, and substrate specificities, have been described. MAO-A preferentially oxidizes nor-epinephrine and serotonin, and is selectively inhibited by clorgyline; whereas MAO-B preferentially deaminates β-phenylethylamine and benzyl-amine, and is selectively inhibited by L-deprenyl.[3]

The two MAO isoforms also have a different tissue distribution; for example, MAO-B is predominant in the human brain, and is compartmentalized into different cell types. It occurs mainly in glial cells and serotoninergic neurons, while MAO-A occurs in cathecholaminergic neurons as well as glia.[4]

Following an initial experience with nonselective, irreversible MAO inhibitors (MAO-Is) in the treatment of depression associated with severe side effects[5] it can be stated that today the new selective, reversible inhibitors of MAO-A and MAO-B are, respectively, useful therapeutic agents in the treatment of depression and anxiety, and coadjuvant agents in the treatment of Parkinson's disease, and perhaps also Alzheimer's disease.[6]

It has been shown recently that MAO is responsible for the biotransformation of 1-methyl-4-phenyl-1,2,3,6-tetrahydropyridine (MPTP) into 1-methyl-4-phenylpyridinium, a Parkinson producing neurotoxin,[7] and may also contribute to the apoptotic process because it inhibits MAO activity-suppressed cell death.[8]

Keywords: MAO-inhibitors; Coumarin.
* Corresponding author. Tel.: +39-06-4991-3763/3975; fax: +39-06-4991-3763; e-mail: daniela.secci@uniroma1.it

0960-894X/$ - see front matter © 2004 Elsevier Ltd. All rights reserved.
doi:10.1016/j.bmcl.2004.05.010

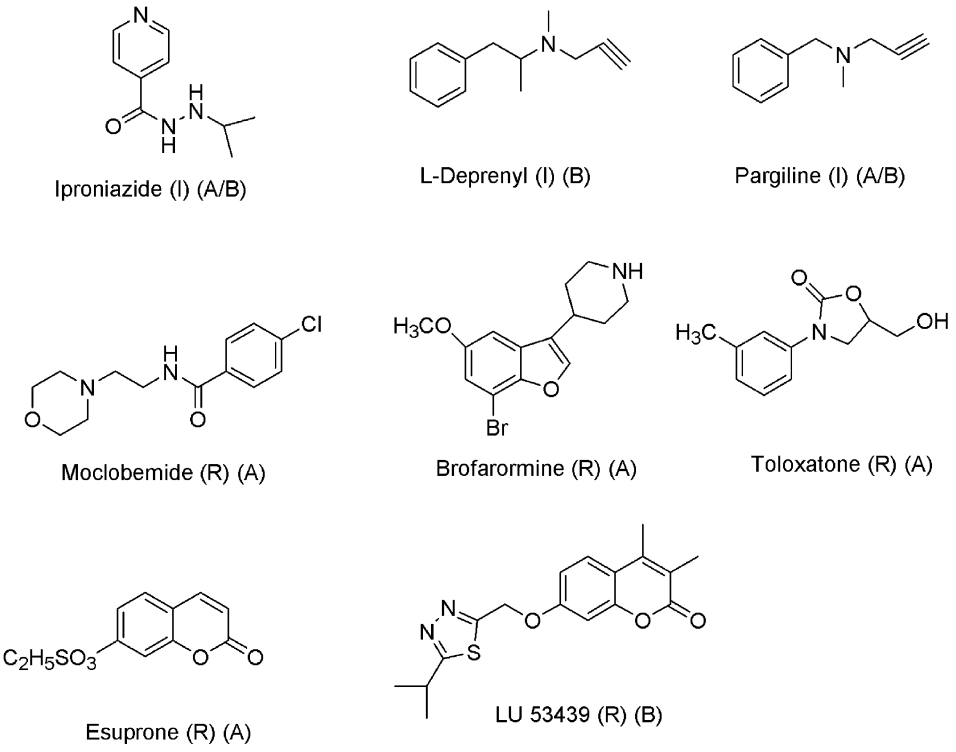

Chart 1. Reversible (R) and irreversible (I) MAO-A/B inhibitors.

Chart 1 shows the structures of the irreversible and nonselective MAO-Is iproniazide[9] and pargyline,[10] of the irreversible and selective MAO-B-I L-deprenyl,[11] of the reversible and selective MAO-A-Is moclobemide, brofaromine and toloxatone,[12] and of other compounds such as esuprone[13] and LU 53439,[14] which are reversible MAO-Is, and selective, respectively, for the A isoform and the B isoform.

That there are many different structures of MAO inhibitors is essentially due to the fact that the active site of the MAOs is unknown. A step forward has been the description of the experimental crystal structure of the human MAO-B active site by Binda et al. in the late 2001.[15] These authors crystallized the pargyline inhibitor covalently bound to the N5 atom on the *re* side of the flavin moiety of the enzyme, identifying the residues bonding the catalytic cavity. Nevertheless, the structure of the active site of MAO-A is still unknown today, limiting the design of new potent selective MAO inhibitors.

Among the different existing inhibitors, those with a (1*H*)-benzopyran structure have been studied recently. Besides esuprone and LU53439 cited above, in recent years 7-benzyloxy coumarin derivatives (Fig. 1) have been reported to have inhibitory activity and selectivity towards MAO-B.[16]

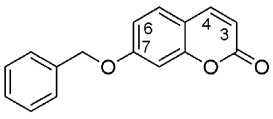

Figure 1. 7-Benzyloxy-coumarin.

It is reported for these compounds that hydrogenation of the 3,4-double bond as well as substitution of the coumarin nucleus at position 3 and/or 4 modulates MAO-B inhibitory activity and A/B selectivity.

Substitution of the coumarin nucleus at position 3 has been carried out with phenyl and methyl groups or with hydrogen, but no data have been reported with polar groups such as acyl so far. Particular attention has been dedicated to the steric hindrance of the substituent at position 6: only small substituents are tolerated. Moreover in the presence of a benzyloxy substituent in the near 7-position, the substituents in the 6-position, methoxy, benzyloxy, glucosyl, or the OH groups decreased or abolished activity, regardless of size or lipophilicity.

Considering that no data was found in the literature on the importance of an acyl in position 3, we deemed it important to study the influence of this group on MAO inhibitory activity and on A/B selectivity. For this reason in this work we synthesized and tested for MAO inhibitory activity some coumarin derivatives substituted at position 3 with carboxylic acid, ethyl ester or acyl chloride groups, at position 6 with halogen, nitro and methyl groups, and unsubstituted at position 7, with the aim of verifying MAO inhibitory activity and A/B selectivity. Since we were dealing with potentially reactive compounds, before carrying out the assays, we tested the chemical stability of the different acyl derivatives in the assay conditions by ^{1}H NMR spectroscopy. Furthermore, we examined the biological results by theoretical methods, by computing several molecular descriptors, including LogP, and considering the binding modes of the most active analogues with respect to

the MAO-B isoform using docking simulations. The results were compared with those of previously reported inhibitors.[17]

2. Chemistry

Coumarins **1a**–**e**, **2b**–**e** (**2a** is commercially available), and **3a**–**e** were synthesized as reported in Scheme 1 and are listed with the analytical data in Table 1.[18–23]

Except for coumarin-3-carboxylic esters **1a**–**e**, obtained following a Knoevenagel reaction between the appropriate benzaldehydes and diethylmalonate, the coumarin nucleus was more conveniently achieved by the heterocyclization reaction of 2-hydroxybenzaldoximes **1 a′**–**e′** and carbon suboxide.[24] This route was preferred in order to afford multigram scale synthesis and easy purification compared with other syntheses.

Oximes **1b′**–**e′** were obtained starting from the appropriate 2-hydroxybenzaldehydes and hydroxylamine. The subsequent reaction with carbon suboxide afforded carboxamides **1b″**–**e″**, which gave acids **2b**–**e** after hydrolysis with sodium hydroxide. Treatment of acids **2a**–**e** with thionyl chloride yielded 3-acyl chlorides **3a**–**e**.

The synthesized compounds were submitted to stability tests in the assay conditions. During the NMR tests, the stability of the esters, of the acids, and of the chlorides was determined in H_2O, DMSO, in a pH 7.4 phosphate buffer, in perchloric acid, and in acetonitrile. In particular the examined samples were held in direct contact at room temperature for 0.5, 1, 2 and 3 h, under stirring with their respective solvent. The NMR spectrum of each quantitatively isolated sample was performed; in the case of the esters and chlorides we looked for the possible appearance of a peak at 13.27 ppm relating to the OH and due to the formation of the corresponding acid, and for all derivatives we looked for the appearance of peaks that were different from those of the initial products.

3. Results and discussion

The stability tests carried out showed that in the assay conditions and in the time provided for (up to 3 h), the assayed compounds were perfectly stable and no

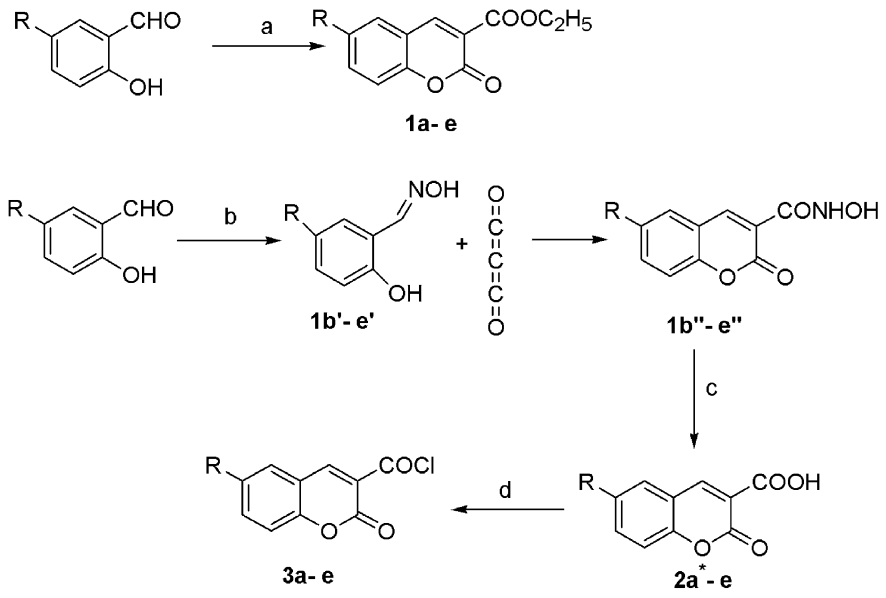

Scheme 1. Reagents and conditions: (a) EtOH, EtOOC–CH_2–COOEt; (b) acetonitrile–water 2:1, NH_2OH hydrochloride, CH_3COONa; (c) NaOH 20%; (d) $SOCl_2$; *__2a__ is commercially available.

Table 1. Chemical–physical data of derivatives **1a**–**e**, **2a**–**e** and **3a**–**e**

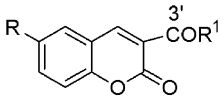

Compound	R	**1** $R^1 = OC_2H_5$		**2** $R^1 = OH$		**3** $R^1 = Cl$	
		Mp (°C)	% Yield	Mp (°C)	% Yield	Mp (°C)	% Yield
a	H	94–96	68	190[a]		130–132	98
b	CH_3	105–106	65	159–160	95	173–175	93
c	Br	162–164	62	200–202	93	158–161	98
d	Cl	145–147	65	280–282	93	163–165	98
e	NO_2	190–192	68	209–212	98	138–140	96

[a] Commercial source.

decomposition or reaction ensued. This allowed to use the acyl derivatives without reserve in order to obtain greater insight on the influence of the carbonyl group on activity. From Table 2,[25] which shows the MAO inhibition data from all the reported compounds, it can be seen that esters **1a**–**e** show weak activity against both MAO isoforms, while acids **2a**–**e** are more active as inhibitors of MAO-B, as their pIC_{50} values range between 7.48 and 7.76. With the exception of 6-nitro coumarin **2e** (pIC_{50} 7.17), the inhibitory activity of these acids against MAO-A was lower (pIC_{50} 4.82–6.30). The introduction of a 6-substituent in coumarin-3-carboxylic acids affects activity against MAO-A. As a matter of fact, it can be observed that activity increases in the substituted compounds (compare the activity of **2a** with that of **2d** and **2e**).

Chlorides **3a**–**e** show high inhibitory activity against MAO-A, as their pIC_{50} values are in the 7.22–7.70 range. These same compounds also show activity against MAO-B, 6-chloro coumarin-3-acyl chloride, **3d**, being the highest ($pIC_{50} = 8.00$).

From this order of activity we can observe that esters are the compounds with the lowest inhibitory activity, and that acids have high potency and B selectivity. In fact compounds **2a** and **2b** (pIC_{50} MAO-B = 7.76 and 7.72, respectively) have a very high selectivity towards the MAO-B isoenzyme (B-selectivity = 2.94 and 2.80, respectively). Acyl chlorides show a high potency against both isoforms.

It is interesting to point out that all assayed compounds act through the reversible mode, as shown by dialysis performed over 24 h in a cold room against a 0.1 M potassium phosphate buffer (pH 7.2) capable of restoring 90–100% of the activity of the enzyme. The proven chemical stability of the acyl derivatives as well as the reversibility of action suggests that the acyl group is involved in the interaction with the enzyme and contributes to its activity.

Table 2. Structures and monoamine oxidase inhibitory activity of derivatives **1a**–**e**, **2a**–**e** and **3a**–**e**[a]

Compound	MAO-A pIC_{50}	MAO-B pIC_{50}	pS.I.[b] selectivity
1a	6.64	5.30	−1.34
1b	6.72	6.00	−0.72
1c	6.68	6.00	−0.68
1d	6.30	6.00	−0.30
1e	6.59	6.00	−0.59
2a	4.82	7.76	2.94
2b	4.92	7.72	2.80
2c	6.00	7.48	1.48
2d	6.30	7.64	1.34
2e	7.17	7.71	0.54
3a	7.22	6.94	−0.28
3b	7.54	7.00	−0.54
3c	7.70	6.96	−0.74
3d	7.52	8.00	0.48
3e	7.54	6.98	−0.56

[a] The data represent mean values of at least three separate experiments.
[b] pS.I.: log selectivity index = pIC_{50}(MAO-B)−pIC_{50} (MAO-A).

The computational work was carried out on a 13-node cluster of Linux Intel 1.5 GHz Pentium IV PCs with the following purposes: (a) to identify physical–chemical properties significantly correlated to the inhibition activities, (b) to study the recognition of the synthesized compounds with the MAO-B enzymatic cleft.

The first computational issue was investigated computing several chemical descriptors. We carried out descriptor analysis with the programs Dragon[29] and ClogP.[30] With Dragon, after generating several hundred molecular descriptors, we found the best linear correlation against the pIC_{50} MAO-B/MAO-A ratio with the Ghose–Crippen method of atom-centred fragments, which qualitatively distinguishes between carboxylic acids (positive values) and ethyl ester or acyl chloride moieties (zero value). In agreement with the selectivity expressed as pIC_{50} ratio, this descriptor was not sufficient to explain our observation of the general lower activity of ester derivatives compared to the compounds of the **2** and **3** series. ClogP values reported in Table 3, generally confirmed the lipophilic trend, which decreased from the ester to the acid and to the chloride derivatives in the homologous series **a**, **b**, **c** and **d**, but could not explain the differences in activity shown in Table 2.

The second computational issue was carried out by docking experiments of these compounds and the only isoform of the enzyme available in the Protein Data Bank (PDB).[15] The crystallographic model, code 1GOS, contains the adduct of the pargyline inhibitor covalently bound to the enzyme isoalloxazine moiety and the residues involved in the catalytic site. According to the MOLINE approach,[31] in the first step in this computational issue was the conformational analysis of each inhibitor by Monte Carlo (MC) simulation with the AMBER* force field united atoms and the GB/SA water implicit solvation model[32] as implemented in the MacroModel program.[33] The acid series of compounds **2a**–**e** was considered in anionic form at physiological pH conditions. The MC search was conducted working only with the isolated compounds sampling all unique conformers within 50 kJ/mol above the global minimum.

In the second step, all MC found conformations for each ligand were submitted to the MOLINE automatic docking procedure.

The receptor was prepared modifying the crystallographic structure of the MAO-B enzyme by removing the pargyline moiety from the 1GOS PDB model. The computational protocol was exactly the same for each compound–enzyme complex.[34]

Table 3. ClogP values for derivatives **1a**–**e**, **2a**–**e** and **3a**–**e**

Compound	R	**1** $R^1 = OC_2H_5$	**2** $R^1 = OH$	**3** $R^1 = Cl$
a	H	1.91	1.54	0.83
b	CH_3	2.77	2.41	1.70
c	Br	2.41	2.04	1.33
d	Cl	2.62	2.26	1.55
e	NO_2	1.65	1.30	0.68

In the third step we analyzed the results of the docking procedure selecting lowest energy bimolecular complexes within 5 kcal/mol above the global minimum. Considering a linear proportionality between the degree of cleft occupation and the inhibitor potency, the inclusion degree of each compound within the enzyme cleft was computed as the probability of finding the ligand in proximity of the FAD isoalloxazine moiety. Using an arbitrary threshold of 10 Å, measured between N5 of this chemical group and C2 of the coumarin moiety, we estimated the percentage of each matching configuration evaluating the degree of cleft occupation for each compound (Table 4). These percentages and the MAO-B pIC_{50} values are in good agreement ($n = 15$, $r^2 = 0.7633$), indicating a higher quality of this 3D descriptor with respect to those adopted in the first issue of the computational work.

Table 4. MAO-B binding modes found by MOLINE within 5 kcal/mol above the global minimum and percentage binding site occupation for series **1**, **2** and **3**

Compound	Number of binding modes	% Binding site occupation
1a	154	14.94
1b	236	1.69
1c	180	2.22
1d	128	4.69
1e	193	0.52
2a	51	96.08
2b	37	97.30
2c	30	100.00
2d	37	94.59
2e	20	95.00
3a	37	97.30
3b	20	100.00
3c	12	100.00
3d	17	100.00
3e	33	18.18

The binding site recognition of the lowest energy configurations obtained in the most active compounds **3d** and **2a** were energy minimized at the same conditions used in the conformational search of each inhibitor. In order to consider the induced fit effect within the binding cleft, a constrained protocol[35] was applied, allowing ligands, FAD, and enzyme residues within 10 Å from the N5 isoalloxazine moiety to relax freely. The geometry of lowest energy complexes of the most active compounds are shown in Figure 2.

Compounds **2a** and **3d** easily fit in the MAO-B active site but with very different binding modes. The acid moiety of compound **2a** is directed towards the cofactor, while the corresponding acid chloride moiety of **3d** is in the opposite position, towards TYR 326. Both compounds shown one hydrogen bond, **2a** with the phenolic hydroxyl of TYR 188 and **3d** with the phenolic hydroxyl of TYR 326.

Substitution of carboxylic hydroxyl with chlorine produces a different hydrogen bond network. In fact, while **2a** showed one hydrogen bond with the phenolic hydroxyl of TYR 188, **3d** established another one with the phenolic hydroxyl of TYR 326. Boltzmann population analysis at 300 °K carried out on all configurations found in the inhibitor–enzyme complex revealed a consistent difference between the two global minima shown in Figure 2. While **2a** is evaluated at 57.60%, demonstrating a large recognition variability within the enzyme cleft, **3d** is much more stable in the binding mode with a population of 94.41%. This different behaviour can be attributed to the stronger steric and electrostatic repulsion between the acyl chloride moiety and GLY 434. Actually, the presence of the chlorine substituent in 6, located in the complex close to GLY 434 and TYR 188, induces the translation of the **3d** coumarin moiety far from these residues, amplifying the differences between the acid and chloride binding modes.

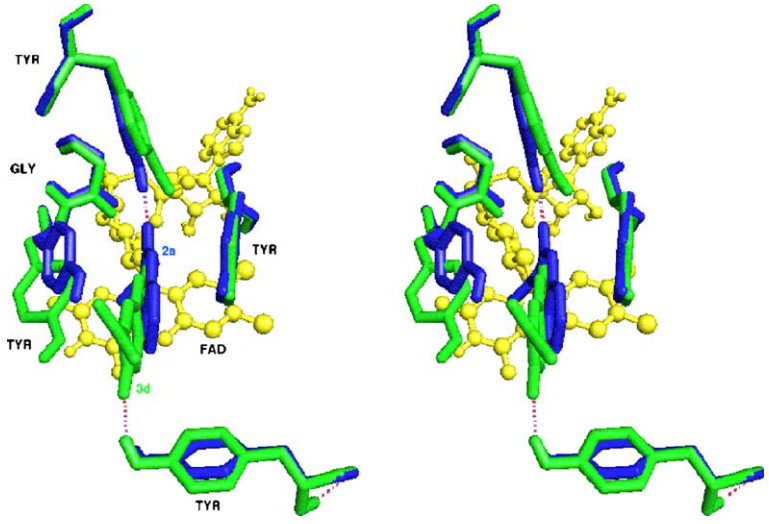

Figure 2. Stereoview comparison of lowest energy MAO-B complexes with **3d** (green polytube model) and **2a** (blue polytube model) within the enzymatic cleft. The cofactor is displayed in ball-and-stick style and the hydrogen bond network in dashed lines. Non-interacting residues with both inhibitors are hidden for clarity.

Comparison of these data with previously reported docking experiments with MAO-B inhibitors[17] confirms the role of residues TYR 345 and TYR 398 as lateral cleft delimitation in the common binding pattern of coumarin and 4,5-dihydro-(1*H*)-pyrazole derivatives. The main difference between the two binding modes is due to the hydrogen bond acceptor contributions of the hydroxyl side chain moieties of TYR 326 and TYR 188, which can only establish productive interactions with coumarin derivatives.

In conclusion, in this work the synthesized coumarin-3-acyl derivatives were tested against MAO-A and MAO-B to assay their potency as inhibitors. Among the tested derivatives we selected coumarin-3-carboxylic acids **2a**–**e** as potent anti-MAO agents, derivatives **2a** and **2b** being highly selective against the MAO-B isoform. Coumarin-3-acyl chlorides **3a**–**e** showed strong anti-MAO activity against both isoforms, especially compound **3d**, which shows the highest activity against MAO-B. Unfortunately this compound showed a very low selectivity index.

The bidimensional molecular descriptors generated in our study cannot fully account for the inhibition of activity and selectivity of our compounds against the MAO-A and B enzymes. 3D descriptors based on the solvent accessible surface qualitatively indicate the role of the steric effect of ester derivatives (which are less active) with respect to acid and chloride compounds (which are more active). MAO-B docking experiments, examined as the probability of occupancy of the enzyme cleft, are crucial to improve the correlation with pIC_{50} and provide binding modes partially corresponding to the interactions found with another series of inhibitors.[17] Availability of the MAO-A crystallographic structure will be necessary to complete the correlation study with selectivity inhibition data.

The information from this study is important for the rational drug design of more potent/selective MAO inhibitors based on the coumarin scaffold.

Acknowledgements

This work was supported by grants from MURST.

References and notes

1. Greenawalt, J. W.; Schnaitman, C. *J. Cell Biol.* **1970**, *46*, 173.
2. Mondovì, B. *Structure and Function of Amine Oxidases*; CRC: Boca Raton, FL, 1985.
3. (a) Johnston, J. P. *Biochem. Pharmacol.* **1968**, *17*, 1285; (b) Weyler, W.; Hsu, Y. P.; Breakefield, O. *Pharmacol. Ther.* **1990**, *47*, 391.
4. (a) Westlund, R. N.; Denney, R. M.; Kochersperger, L. M.; Rose, R. M.; Abell, C. W. *Science* **1983**, *219*, 979; (b) Geha, R. M.; Rebrin, I.; Chen, K.; Shih, J. C. *J. Biol. Chem.* **2001**, *276*, 9877.
5. Anderson, M. C.; Hasan, F.; McCrodden, J. M. *Neurochem. Res.* **1993**, *18*, 1145.
6. Wouters, J. *Curr. Med. Chem.* **1998**, *5*, 137.
7. (a) Chiba, K.; Trevor, A.; Castagnoli, N. *Biochem. Biophys. Res. Commun.* **1984**, *120*, 574; (b) Fritz, R. R.; Abell, C. W.; Patel, N. T.; Gessner, W.; Brossi, A. *FEBS Lett.* **1985**, *186*, 224; (c) Grimsby, J.; Toth, M.; Chen, K.; Kumazawa, T.; Klaidman, L.; Adams, J. D.; Karoum, F.; Gal, J.; Shih, J. C. *Nat. Genet.* **1997**, *17*, 1.
8. De Zutter, G. S.; Davis, R. J. *Proc. Natl. Acad. Sci. U.S.A.* **2001**, *98*, 6168.
9. Mc Millan et al. *J. Am. Pharm. Assoc., Sci. Ed.* **1953**, *42*, 457.
10. Fowler, C. J.; Oreland, L.; Callingham, B. A. *J. Pharm. Pharmacol.* **1981**, *33*, 341.
11. Knoll, J.; Ecsery, Z.; Kelemen, K.; Nievel, J.; Knoll, B. *Arch. Int. Pharmachodyn. Ther.* **1965**, *155*, 154.
12. (a) Moureau, F.; Wouters, J.; Vercauteren, D. P.; Collin, S.; Evrard, G.; Durant, F.; Ducrey, F.; Koenig, J. J.; Jarreau, F. X. *Eur. J. Med. Chem.* **1992**, *27*, 939; (b) Moureau, F.; Wouters, J.; Vercauteren, D. P.; Collin, S.; Evrard, G.; Durant, F.; Ducrey, F.; Koenig, J. J.; Jarreau, F. X. *Eur. J. Med. Chem.* **1994**, *29*, 269; (c) Moureau, F.; Wouters, J.; Depas, M.; Vercauteren, D. P.; Durant, F.; Ducrey, F.; Koenig, J. J.; Jarreau, F. X. *Eur. J. Med. Chem.* **1995**, *30*, 823; (d) Rabasseda, X.; Sorbera, L. A.; Castaner, J. *Drugs Future* **1999**, *24*, 1057; (e) Wouters, J.; Moureau, F.; Evrard, G.; Koenig, J. J.; Jegham, S.; George, P.; Durant, F. *Bioorg. Med. Chem.* **1999**, *7*, 1683.
13. Bergström, M.; Westerberg, G.; Nemeth, G.; Traut, M.; Gross, G.; Greger, G.; Müller-Peltzer, H.; Safer, A.; Eckernäs, S. A.; Grahner, A.; Langström, B. *Eur. J. Clin. Pharm.* **1997**, *52*, 121.
14. Loscher, W.; Lehmann, H.; Teschendorf, H. J.; Traut, M.; Gross, G. *J. Pharm. Exper. Therap.* **1999**, *288*, 984.
15. Binda, C.; Newton-Vinson, P.; Hubalek, F.; Edmondson, D. E.; Mattevi, A. *Nat. Struct. Biol.* **2002**, *9*, 22.
16. Gnerre, C.; Catto, M.; Leonetti, F.; Weber, P.; Carrupt, P. A.; Altomare, C.; Carotti, A.; Testa, B. *J. Med. Chem.* **2000**, *43*, 4747.
17. Manna, F.; Chimenti, F.; Bolasco, A.; Secci, D.; Bizzarri, B.; Befani, O.; Turini, P.; Mondovi, B.; Alcaro, S.; Tafi, A. *Bioorg. Med. Chem. Lett.* **2002**, *12*, 3629.
18. Jitendra, R. H.; Susheel, J. N.; Manikrao, M. S. *Tetrahedron Lett.* **2002**, *43*, 1127.
19. Bonsignore, L.; De Logu, A.; Lavagna, S. M.; Loy, G.; Secci, D. *Eur. J. Med. Chem.* **1994**, *29*, 479.
20. Pochet, L.; Doucet, C.; Schynts, M.; Thierry, N.; Boggetto, N.; Pirotte, B.; Jiang, K. Y.; Masereel, B.; de Tullio, P. *J. Med. Chem.* **1996**, *39*, 2579.
21. Doucet, C.; Pochet, L.; Thierry, N.; Pirotte, B.; Delarge, J.; Reboud-Ravaux, M. *J. Med. Chem.* **1999**, *42*, 4161.
22. Bonsignore, L.; Cottiglia, F.; Lavagna, S. M.; Loy, G.; Secci, D. *Heterocycles* **1999**, *50*, 469.
23. Ji, M.; Hua, W.; Wu, X.; Duan, T. *Zhongguo Yaoke Daxue Xuebao* **1988**, *19*, 241.
24. Bonsignore, L.; Cottiglia, F.; Lavagna, S. M.; Loy, G.; Secci, D. *Il Farmaco* **1998**, *53*, 693, and references cited therein.
25. All chemicals were commercial reagents of analytical grade and were used without purification. Bovine brain mitochondria (MAO) were isolated according to Basford.[26] In all experiments the AO activities of the beef brain mitochondria were determined by a fluorimetric method, according to Matsumoto et al.[27] using kinuramine as a substrate at four different final concentrations ranging from 5 μM to 0.1 mM. Briefly, the incubation mixtures contained: 0.1 mL of 0.25 M potassium phosphate buffer (pH 7.4), mitochondria (6 mg/mL) and drug solutions with a final concentration ranging from 0 to 10^{-3} μM.

The solutions were incubated for 30 min at 38 °C; addition of perchloric acid ended the reaction. The samples were centrifuged at 10,000/5 min and the supernatant was added up to 2.7 mL of NaOH 0.1 N. Coumarin derivatives were dissolved in dimethyl-sulfoxide (DMSO), which was added to the reaction mixture from 0 to 10^{-3} μM. In order to study the inhibition of coumarin derivatives on the activities of both MAO-A and B separately, the mitochondrial fractions were pre-incubated for 30 min at 38 °C before adding the specific inhibitors (L-deprenyl 0.5 μM to estimate MAO-A activity, and clorgyline 0.05 μM to assay the isoform B), considering also that MAO-A is irreversibly inhibited by a low concentration of clorgyline, but is unaffected by a low concentration of L-deprenyl, which on the contrary is used in the MAO-B form. Fluorimetric measurements were recorded with a Perkin–Elmer LS 50B Spectrofluorimeter. The protein concentration was determined according to Bradford.[28] The results are reported in Table 2. The data are the means of three or more experiments each performed in duplicate.

26. Basford, R. E. *Methods Enzymol.* **1967**, *10*, 96.
27. Matsumoto, T.; Suzuki, O.; Furuta, T.; Asai, M.; Kurokawa, Y.; Rimura, Y.; Katsumata, Y.; Takahashi, I. *Clin. Biochem.* **1985**, *18*, 126.
28. Bradford, M. M. *Anal. Biochem.* **1976**, *72*, 248.
29. Dragon ver. 3.0, 2003, Talete s.r.l., Milan, Italy.
30. ClogP ver 4.81, 2003, Daylight Chemical Information Systems, Inc. Mission Viejo, 92691 California, USA.
31. Alcaro, S.; Gasparrini, F.; Incani, O.; Mecucci, S.; Misiti, D.; Pierini, M.; Villani, C. *J. Comput. Chem.* **2000**, *21*, 515–530.
32. Still, W. C.; Tempczyk, A.; Hawley, R. C.; Hendrickson, T. *J. Am. Chem. Soc.* **1990**, *112*, 6127.
33. Macromodel Linux ver. 7.2 Mohamadi, F.; Richards, N. G. J.; Guida, W. C.; Liskamp, R.; Lipton, M.; Caufield, C.; Chang, G.; Hendrickson, T.; Still, W. C. *J. Comput. Chem.* **1990**, *11*, 440–467.
34. According to the MOLINE methodology and previously reported enzyme–ligand docking experiments, both grid resolution GR and Van der Waals compression factor χ were established at 6 and 0.8, respectively. The adopted resolution generated exactly 65,712 configurations for each inhibitor–enzyme complex. Other docking protocol details are the activation of the selection module: SEL_5FD, and the number of cycles of the rigid optimization process: 3, each with 100 Simplex iterations. The force field used for the protocol validation was AMBER* united atoms with dielectric constant 80.
35. In the constrained protocol two different shells of atoms were generated. One included all atoms located between 10 and 12 Å from FAD N5, on which a constant force of 100 kJ/mol was applied to the coordinates in order to limit the freedom of moments. The other shell included the enzyme atoms 'frozen' (rigidly fixed and not considered in the energy evaluation) more than 12 Å from the isoalloxazine moiety.